AD A119135

㎜. FILE COPY

⑩

DOCUMENT CONTROL DATA - R & D

(Security classification of title, body of abstract and indexing annotation must be entered when the overall report is classified)

1. ORIGINATING ACTIVITY *(Corporate author)*	2a. REPORT SECURITY CLASSIFICATION
Department of Metallurgy & Mining Engineering University of Illinois Urbana, IL 61801	Unclassified
	2b. GROUP

3. REPORT TITLE

Photoelastic Investigation of the Double Torsion Specimen

4. DESCRIPTIVE NOTES *(Type of report and inclusive dates)*

Technical

5. AUTHOR(S) *(First name, middle initial, last name)*

B. Hindin

6. REPORT DATE	7a. TOTAL NO. OF PAGES	7b. NO. OF REFS
August 1982	29	13

8a. CONTRACT OR GRANT NO.	9a. ORIGINATOR'S REPORT NUMBER(S)
N00014-75-C-1012 b. PROJECT NO.	
c.	9b. OTHER REPORT NO(S) *(Any other numbers that may be assigned this report)*
d.	

10. DISTRIBUTION STATEMENT

This document is unclassified. Distribution and reproduction for any purpose of the U.S. government is permitted.

11. SUPPLEMENTARY NOTES	12. SPONSORING MILITARY ACTIVITY
	Office of Naval Research Arlington, Virginia

13. ABSTRACT

The stress distribution of the double-torsion fracture mechanics specimen geometry is presented using a photelastic "frozen stress" technique. Isochromatic fringes of a plastic double-torsion specimen under load were photographed and analyzed in the top, middle and bottom planes parallel to the top surface. Principal stress directions for these planes are also given. The relative magnitudes of the principal stresses perpendicular to the crack plane at the crack tip, crack origin and a point midway between the origin and crack tip are shown.

DTIC
SELECTED
SEP 1 3 1982
H

DISTRIBUTION STATEMENT A

Approved for public release;
Distribution Unlimited

DD FORM NOV 65 1473

82 08 26 010

14 KEY WORDS	LINK A		LINK B		LINK C	
	ROLE	WT	ROLE	WT	ROLE	WT
Double Torsion Specimen						
Fracture Mechanics						
Photelasticity						
Stresses						
Elasticity						

PHOTOELASTIC INVESTIGATION OF THE DOUBLE TORSION SPECIMEN

B. Hindin

Technical Report

USN 00014-75-C-1012

August 1982

Submitted by:

Howard K. Birnbaum

However, no analysis of the stress distribution in the DT specimen by photoelastic techniques appears in the literature.

This investigation was undertaken in order to document the stress distribution in the plane of the DT specimen. The following analysis is intended to give the relative magnitude of the projected principal stresses in the top, middle and bottom sections of the specimen.

THEORY

A brief discussion on the theory of photoelasticity is given in the following paragraphs. A more complete treatment can be found elsewhere [9-11].

The utility of the photoelastic technique is based upon transparent isotropic solids becoming birefringent when subjected to a uniaxial stress. This results in the polarization of light transmitted through the solid with the axes of the polarized light being parallel to the directions of the principal stresses in the solid. Birefringence of the stressed solid also results in a velocity retardation of one polarized wave front with respect to the other. This retardation is proportional to the stress and to the thickness of the solid transversed by the light. The relative retardation can be measured by the phenomenon of interference and can best be observed using plane polarized, monochromatic light.

There are two conditions that will produce destructive interference of transmitted polarized light. One is when the relative retardation is equal to an exact multiple of wavelengths and the second is when the principal stresses in the solid are parallel to the polarizer and analyzer, respectively. The first condition produces 'isochromatic fringes' while the second condition produces 'isoclinic lines' (or fringes). From these observations one can

determine the directions of the principal stresses and the differences of the principal stresses at every point in the specimen.

The preceeding discussion assumes that generalized plan stress conditions exist in the specimen. In a specimen containing triaxial stresses, the principal stress directions and magnitudes will change with thickness. In these cases, the "frozen stress" technique discussed below is used to allow a three dimensional specimen to be analyzed as a series of two dimensional specimens under plane stress conditions. The "frozen stress" technique is normally reserved for analyzing the stress distribution of complicated configurations. Though the DT specimen is in the shape of a simple rectangular plate, Fig. 1, the loading arrangement produces a triaxial stress distribution through the specimen's thickness and the "frozen stress" technique was used.

EXPERIMENTAL PROCEDURE

The DT specimen used in this study was machined from precast epoxy resin type PSM-9[**]. By using this polymer and the proper load-thermal cycle described further on, the fringe pattern from an applied stress can be "frozen" into the model. The model can subsequently be cut into thin slices, without altering the fringe pattern, and examined as a generalized plane stress model.

As discussed by Hendry [9] the phenomenon of stress freezing is due to the existence of two phases in the plastic. One is very temperature dependent being rigid at room temperature and fluid at high temperature. The other phase has a small temperature dependency and is rigid at all temperatures but

[**]Obtained from Photoelastic Division, Measurements Group, Raleigh, NC.

less so than the low temperature rigidity of the first phase. A mechanical model consisting of a spring in a fluid which is rigid at room temperature but fluid at the softening temperature represents the stress freezing quite well.

The plastic DT specimen was 10.2 mm thick, 56 mm wide, and 120 mm long. A notch 32 mm long on top and 40 mm on bottom of the specimen was cut with a jeweler's saw. After machining, the specimen was placed in an Instron loading stage and immersed in an inert silicone oil bath. Heating and cooling rates were controlled by passing the current from a clock driven variable transformer to a 400 W heater. Temperature was monitored by thermocouples and kept uniform by circulating the oil. The heating rate was 150 K/hr. At a final temperature of 403 K, a compressive load of 10 N was applied to the specimen. This was sufficient to initiate a crack. While maintaining this load, the specimen was annealed for 2 hours at 403 K. The temperature was then lowered to room temperature at a rate of 2 K/hr.

After the stress freezing cycle, the specimen was sliced in the manner shown in Fig. 2 using a water cooled jeweler's saw to minimize generation of heat which would tend to distort the fringe pattern at the cut edges. The slices consisted of six squares 33 mm on a side, corresponding to 60% of the specimen width. The actual thicknesses are listed in Table I. Cut surfaces were wet sanded to minimize surfaces scratches. Slices 1 and 4 represent the top surface of the specimen, 2 and 5 the middle and 3 and 6 the bottom. Slices 2 and 3 each consisted of two halves, since the propagating crack bisected them. Slices 1, 5 and 6 were partially bisected.

A circular polariscope was used to observe the isochromatics and isoclinics with a fringe multiplier used to obtain reasonable numbers of observable isochromatics. Only a multiplication of five, however, was attainable before off-axis distortion prevented the resolution of higher order

fringes. All isochromatics were photographed in bright field on Kodak's
Contrast Process Ortho 4154 film using monochromatic lights from a green
filtered mercury lamp. Isoclinics were photographed on PN 55 Polaroid film
using a diffuse fluorescent light source. Isoclinics for the middle section,
slices 2 and 5, were difficult to locate and their positions for angles
between 40° and 90° had to be estimated. The middle section only exhibited
two orders of isochromatics even under fringe multiplication of five.

RESULTS

1. Model Fringe Value Calculation

A measurement of the material stress fringe for PSM-9 was necessary
before the principal stress differences could be calculated from the
isochromatics. The fringe value is defined as the stress required to produce
N number of fringes in a plate of thickness t and is given by [10]:

$$f = (\sigma_1 - \sigma_2)t/N \qquad (2)$$

where σ_1 and σ_2 are the principal stresses.

A calibration disk with a diameter of 53.9 mm was loaded in compression
along a diameter to find the f value. The thermal cycle of the disk was
controlled to closely duplicate the thermal cycle of the DT model.
Isochromatics of the disk were photographed, without a fringe multiplier, in
green monochromatic light. Both bright and dark field were used in order to
obtain one half fringe resolution. Figure 3 shows the bright field
isochromatic fringes of the calibration disk. The analytical expression for
the principal stress differences at the center of the disk is given by [11]:

$$\sigma_1 - \sigma_2 = 8P/\pi dt \qquad\qquad (2)$$

where   P = applied compressive load

d = diameter of disk

At the center of the disk, for an applied compressive load of 32.5 N, the fringe order was found to be 4.8 using a fifth order fringe multiplier. The actual fringe value was calculated to be (4.8/5) = 0.96. Using equation (1) and (2), the material fringe value for the photoelastic material was found to be

$$f_{slice} = 6.40 \times 10^4 \text{ Pa·mm·fr}^{-1} \qquad\qquad (3)$$

The model fringe values given by F = f/t for the slices are listed in Table I.

2. Principal Stress Differences and Directions

In this section, the isochromatics and isoclinics for the top, middle and bottom slices are given. The principal stress directions are drawn for the isoclinics (using the methods of Jessop and Harris [12]), and the ratios of the principal stress differences for several selected directions through the slices are compared. Ratios instead of the actual stress difference values were presented to facilitate comparison of the slices. It is important to note that the calculated principal stress differences are not the principal stress differences but instead projections of the principal stress differences in the plane of the slices. With the information given below, it is not possible to resolve the stress differences into their principal components. A comprehensive solution to the stress distribution in the DT specimen would require a second identically prepared plastic DT specimen model whose slices were perpendicular to the original six. Then, in theory, the principal stress

differences could be resolved into their individual components. Since these stresses were not resolved in this study, this analysis should be used only for comparing relative magnitudes of plane stress differences as a function of specimen thickness.

Figures 4-6 show the isoclinics and stress trajectories. Since the slices as well as the entire specimen are symmetrical about the plane of the crack surface, the isoclinics are drawn on the left half and the principal stress directions are drawn on the right half for clarity of presentation.

Figures 7-9 show the optical photograph of the isochromatic fringes of the top, middle and bottom slices, respectively. Since the isochromatics shown in Figs. 7-9 are composite pictures made up of up to three sections, each having slightly different thicknesses, the fringe pattern does not line up exactly at all places. To facilitate analysis of these fringe patterns, curve smoothing techniques were applied to the isochromatic photographs. These are shown in Figs. 10-12 for the top, middle and bottom slices, respectively.

All curves represent odd half numbers of relative wavelength retardation and are labeled for fringe order where space allowed. Also drawn on the right half of these isochromatic figures are three parallel lines labeled OA, OB and OC which lie perpendicular to the crack direction. Each line is graduated in fractional units of one half the width, W of the specimen. The line OA intersects the crack tip on the bottom slice, OC intersects the crack origin on the top slice and OB intersects the fracture surface on the top, bottom and middle. It is of interest to examine how the relative magnitude of the principal stress difference varies along lines OA, OB and OC for the three different levels.

Figures 13-15 show the ratio of the principal stress difference as a

function of the distance along lines OA, OB and OC, respectively. For each figure the ordinate is normalized with respect to the minimum stress occurring at point O along either OA, OB or OC. For example, in Fig. 14 at the origin of line OB, the principal stress difference of the bottom slice is 3.5 times greater than at the middle slice. These results are discussed below.

The approximate state of stress near the crack front can be recognized by considering the loading arrangement of the DT specimen. Thus, the crack front appearing on the top surface should be in a state of compression. The crack surface in the middle section should be in a neutral stress zone, similar to the neutral plane which occurs in a beam loaded in pure bending. On the bottom of the specimen, the crack surface should be in a state of tension.

Referring to Fig. 13, the principal stress difference along OA intersects the crack tip in the bottom surface and therefore exhibits the greatest stress concentration. While the fractional orders of the isochromatics intersection OA for the middle section were too ill defined to locate, they were substantially less than the stresses at the top or bottom sections. The principal stress difference at the leading edge of the crack front on the bottom surface which corresponds to the origin of line OA on the bottom surface, is greater than at the leading edge of the crack on the top surface by a factor of at least 3.0. In Fig. 14, the principal stress differences occurring along OB are also greatest for the bottom. The stresses in the middle were again less than those for top or bottom. In particular, the stresses at the origin of OB in the bottom and top sections were factors of 3.5 and 1.3, respectively greater than for the middle section. As shown in Fig. 15, the principal stress differences along line OC are greatest for the top section especially close to the crack surface. This is understandable since line OC is perpendicular to the intersection of the crack surface with

the top surface. The stresses along OC in the middle section are less than at the top and bottom sections but not as small as in the cases for lines OA and OB. At the trailing edge of the crack, which corresponds to the origin of line OC, the principal stress difference is a maximum for the top surface where the value is a factor of 1.5 greater than the principal stress difference at the bottom and a factor of 2.7 greater than the stress difference in the middle section.

Experimental data has suggested that the crack front is predominantl Mode I Opening [13]. As shown in Fig. 6, one of the principal stress directions is almost perpendicular to the fracture surface at the crack t It has been shown that this as a tensile stress, implying a Mode I loading is occurring. This would then justify the use of Mode I stess intensity factor, K_I in fracture mechanics calculations for the DT specimen.

SUMMARY

The analysis presented provides a means of comparing the relative magnitudes of the stresses in the DT specimen. Within specific dimensional constraints (which are described elsewhere [1,5]) the results of this investigation are applicable to most other DT specimens. The stress distribution in the immediate vicinity of the crack tip in metal DT specimens may differ slighly from the distribution shown here due to the presence of a plastic zone. The far field stress distribution in a metal specimen, however, should be very similar to the elastic stress distributions shown in this investigation. Ceramic and glass DT specimens, as well as other plastic specimens kept within elastic behavior, should have nearly identical stress distributions to those shown here.

ACKNOWLEDGEMENTS

REFERENCES

1. E. R. Fuller, Jr., An Evaluation of Double-Torsion Testing - Analysis, Fracture Mechanics Applied to Brittle Materials. ASTM STP 678. S. W. Freiman, Ed. American Society for testing Materials, 1979, 3-18.

2. B. J. Pletka, E. R. Fuller, Jr. and B. G. Koepke, An Evaluation of Double-Torsion Testing - Experimental, ibid., 19-37.

3. F. P. Champomier, Crack Propagation Measurements on Glass: A Comparison Between Double-Torsion and Double-Cantilever Beam Specimens, ibid., 60-72.

4. A. V. Virkar and D. L. Johnson, Some Kinetic Considerations Regarding the Double-Torsion Specimen, J. Am. Ceram. Soc., 59, No. 5-6, 197-206 (1976).

5. G. G. Trantina, Stress Analysis of the Double-Torsion Specimen, J. Am. Ceram. Soc., 60, No. 7-8, 338-341 (1977).

6. J. C. Pollet and S. J. Burns, Crack Velocity Correction Factor for the Crack-Front Shape in Double-Torsion Specimens, J. Am. Ceram. Soc., 62, No. 7-8, 426-427 (1979).

7. A. V. Virkar and R. S. Gordon, Crack Front Profiles in Double-Torsion Specimens, J. Am. Ceram. Soc., 58, No. 11-12, 536-537 (1975).).

8. D. K. Shetty, Anil V. Virkar and M. B. Harward, Crack Front Shape Corrections for Crack Velocities in Double-Torsion Specimens, J. Am. Ceram. Soc., 62, No. 5-6, 307-309 (1979).

9. A. W. Hendry, Elements of Experimental Stress Analysis, S. I. Edition, Pergamon Press, Oxford, 97 (1977).

10. A. J. Durelli and W. F. Riley, Introduction to Photomechanics, Prentice-Hall, Inc., Englewood Cliffs, NJ, 64 (1965).

11. S. P. Timoshenko and J. N. Goodier, Theory of Elasticity, Third Edition, McGraw Hill, NY, 167 (1970).

12. H. T. Jessop and F. C. Harris, Photoelasticity, Principles and Methods, Dover, NY, 73 (1960).

13. A. G. Evans, A Method for Evaluating the Time Dependent Failure Characteristics of Brittle Materials - and Its Application to Polycrystalline Alumina, J. Mater. Sci., 7, 1137-1146 (1972).

Table I

MODEL FRINGE VALUES FOR THE SLICES OF THE DT SPECIMEN

Slice	Slice Thickness, t (mm)	Model Fringe Value, F (Pa/fringe)
Top	2.34	2.74×10^4
Middle	2.41	2.66×10^4
Bottom	2.28	2.81×10^4

FIGURE CAPTIONS

Figure 1.   Loading arrangement of plastic DT specimen.

Figure 2.   Exploded view of plastic DT specimen showing slices used in
            photoelastic analysis.

Figure 3.   Bright field isochromatic fringes of the calibration disk exposed
            to green monochromatic light. Applied compressive diametrical
            load was 32.5 N and disk thickness was 10.2 mm.

Figure 4.   Isoclinics (dashed curves) and lines of principal stresses (solid
            curves) for top slices (1 and 4).

Figure 5.   Isoclinics (dashed curves) and lines of principal stresses (solid
            curves) for middle slices (2 and 5).

Figure 6.   Isoclinics (dashed curves) and lines of principal stresses (solid
            curves) for bottom slices (3 and 6).

Figure 7.   Optical photograph of the isochromatic fringes of the top slices
            Nos. 1 and 4.

Figure 8.   Optical photograph of the isochromatic fringes of the middle
            slices Nos. 2 and 5.

Figure 9.   Optical photograph of the isochromatic fringes of the bottom
            slices Nos. 3 and 6.

Figure 10. Isochromatic fringes for top slices (1 and 4). Lines OA, OB and
            OC are graduated in tenths of (W/2).

Figure 11. Isochromatic fringes for middle slices (2 and 5). Lines OA, OB
            and OC are graduated in tenths of (W/2).

Figure 12. Isochromatic fringes for bottom slices (3 and 6). Lines OA, OB
            and OC are graduated in tenths of (W/2).

Figure 13. Principal stress difference ratio versus distance along OA from

crack front

$W = 56.0$ mm
$W_m = 17.5$ mm
$L = 120$ mm
$T = 10.2$ mm
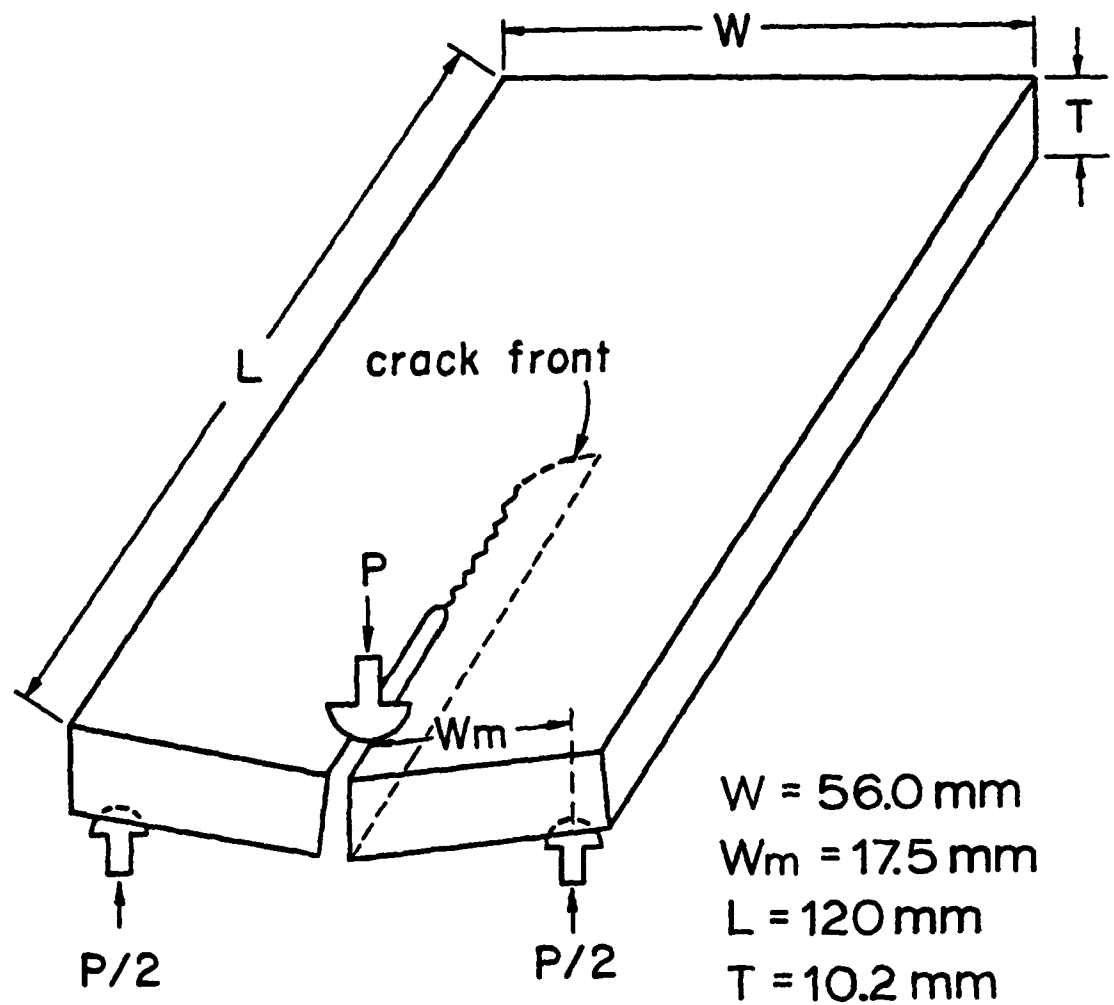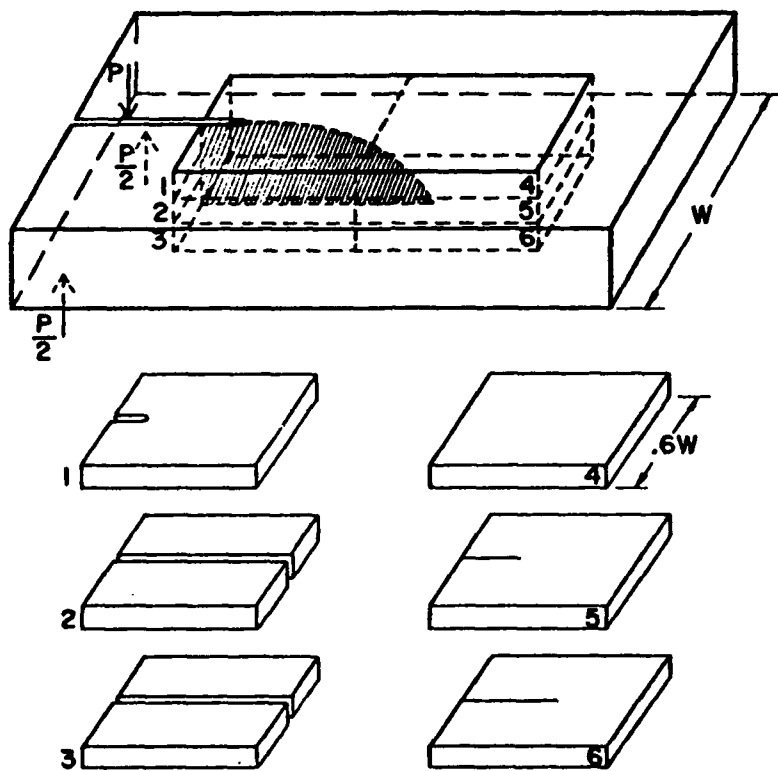
Fig. 1 B. Hindin

Fig. 2   B Hindin

Fig. 3 B Hindin

30° 20° 10°

40°
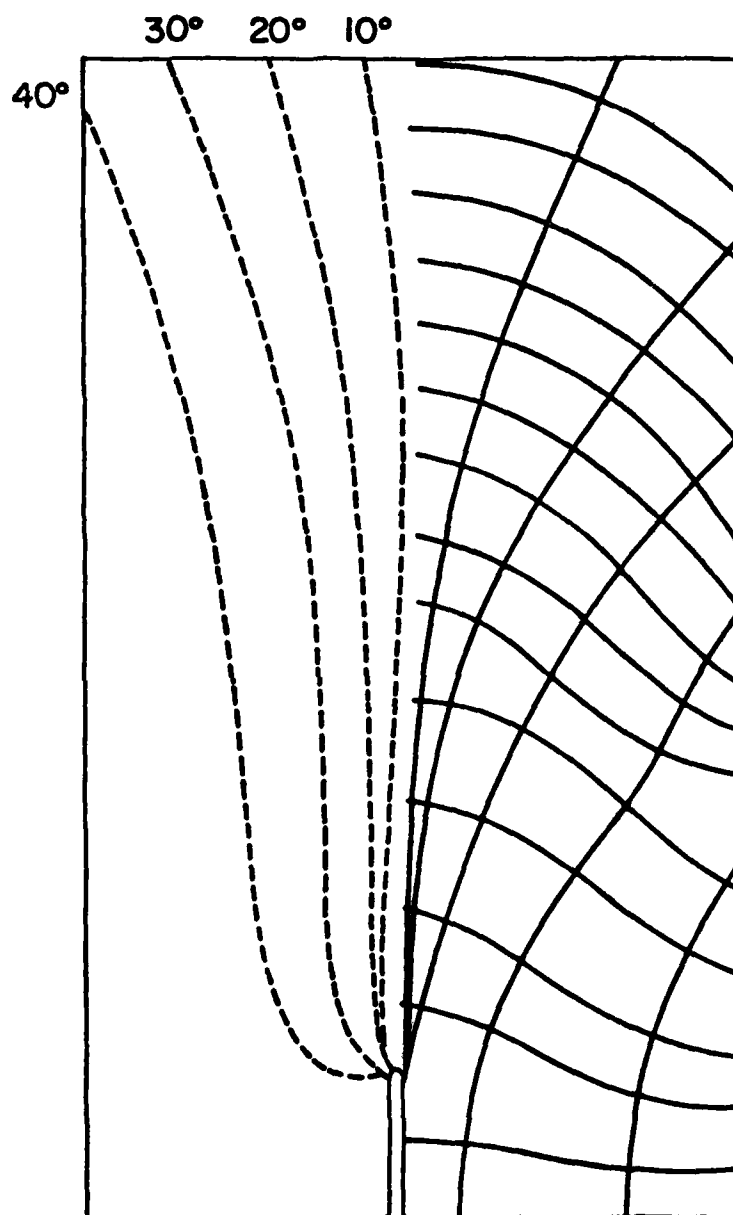
Fig. 4   B. Hindin

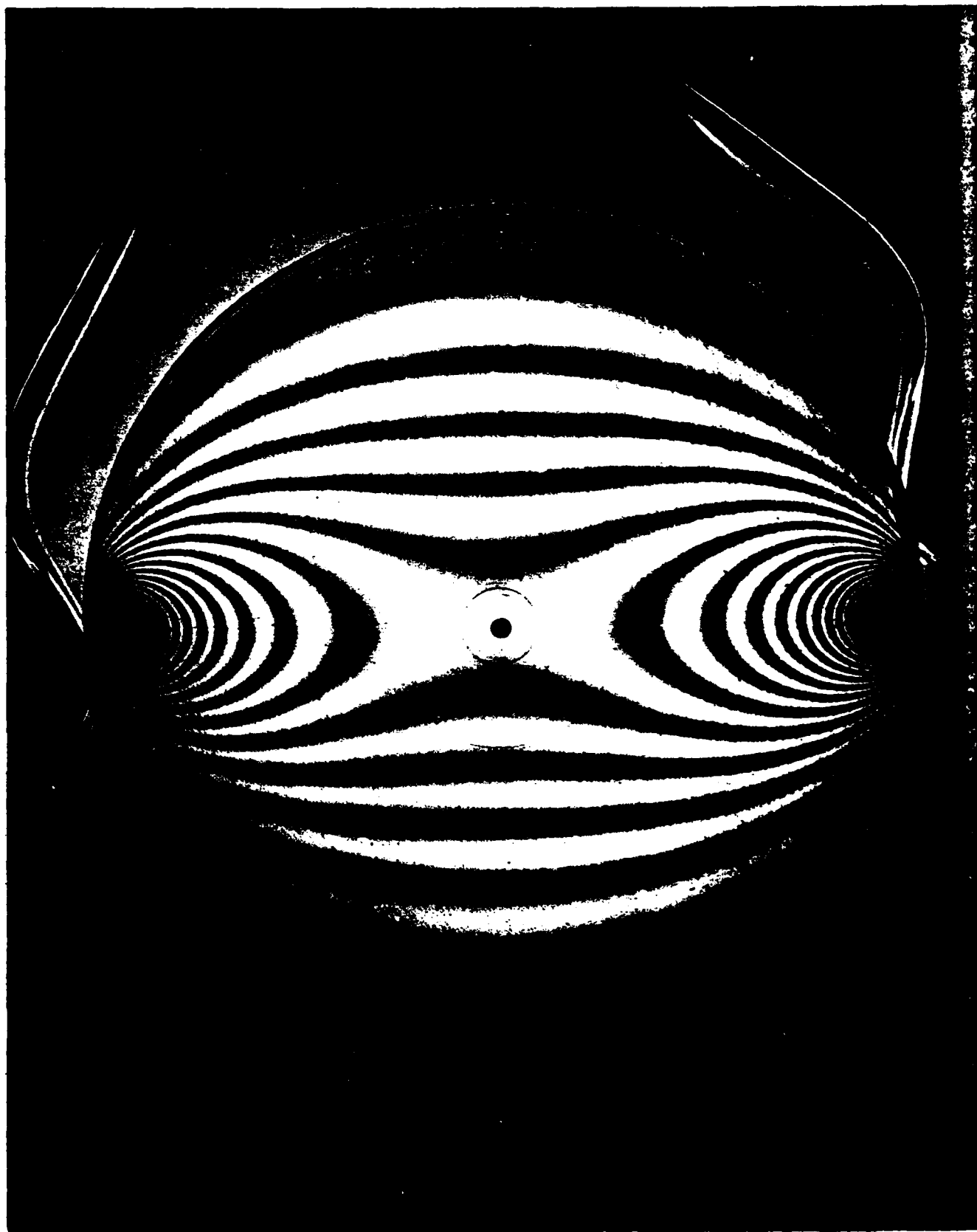Fig. 5 B. Hindin

Fig. 6 B. Hindin

A

Fig. 7   B. Hindin

Fig. 8 B. Hindin

Fig. 9   B. Hindin

Fig. 10   B. Hindin

Fig. 11   B. Hindin
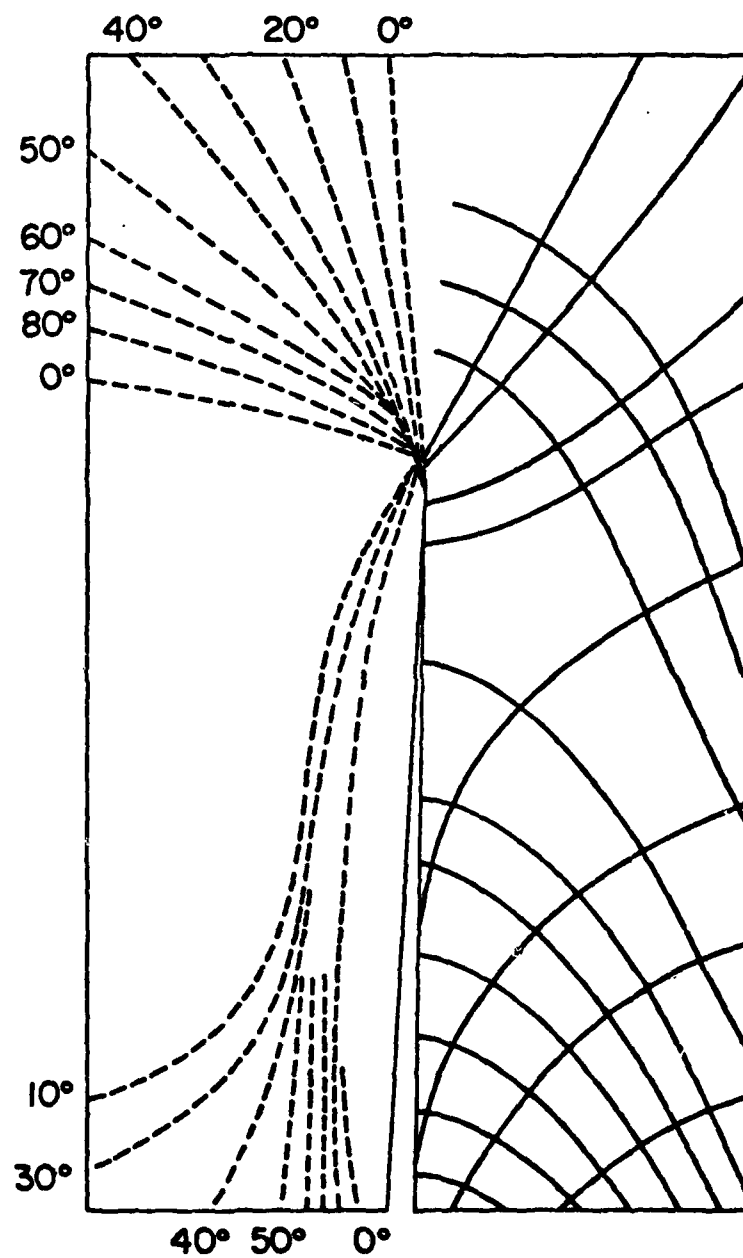
Fig. 12   B. Hindin
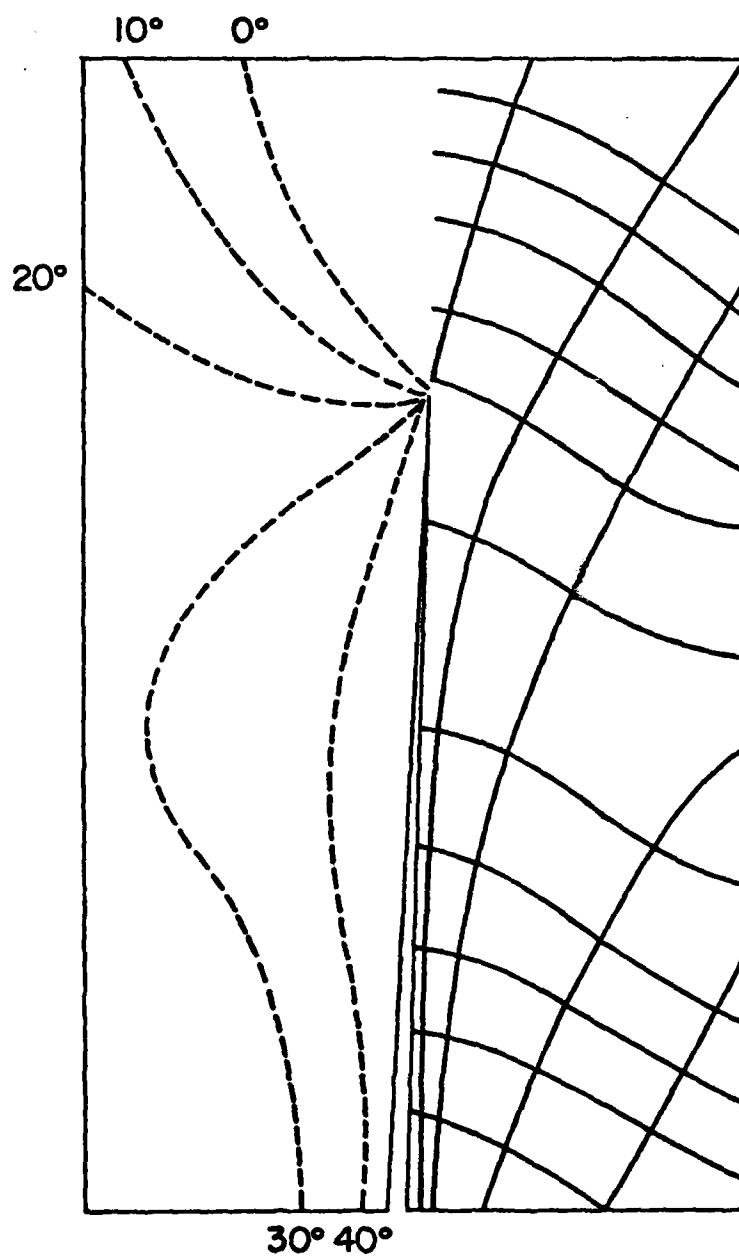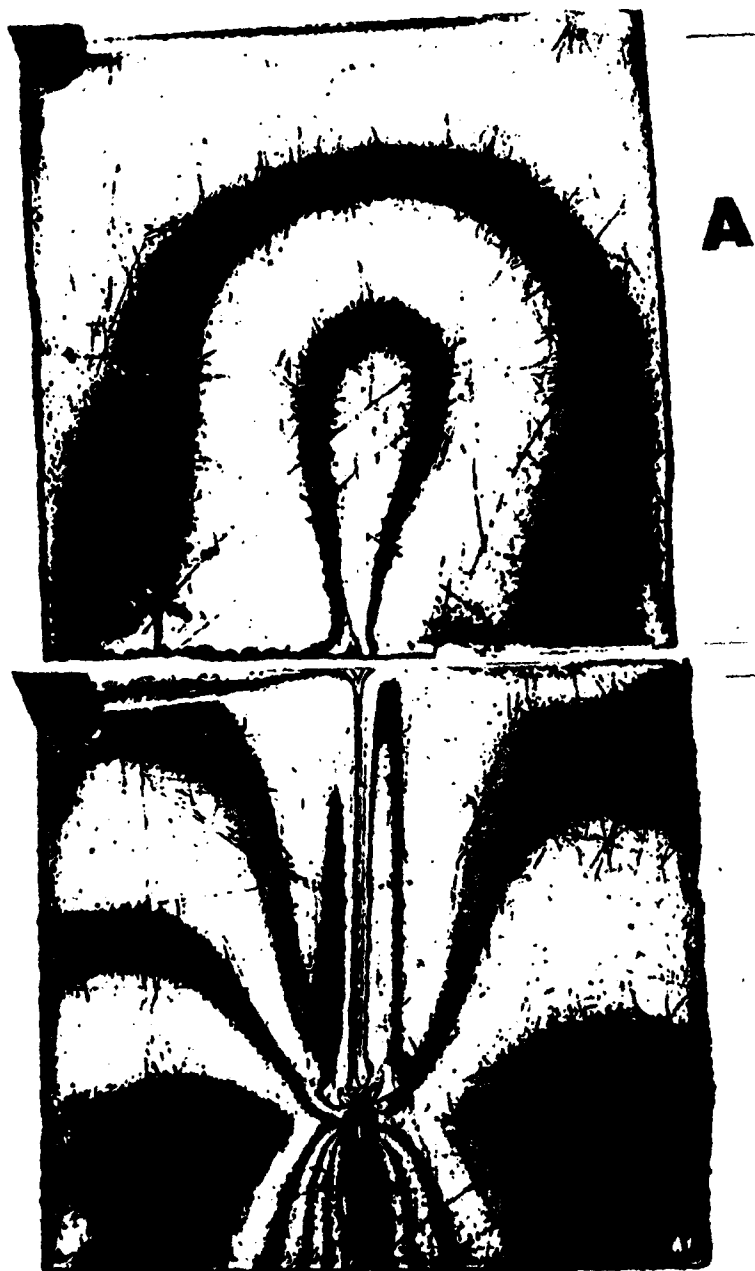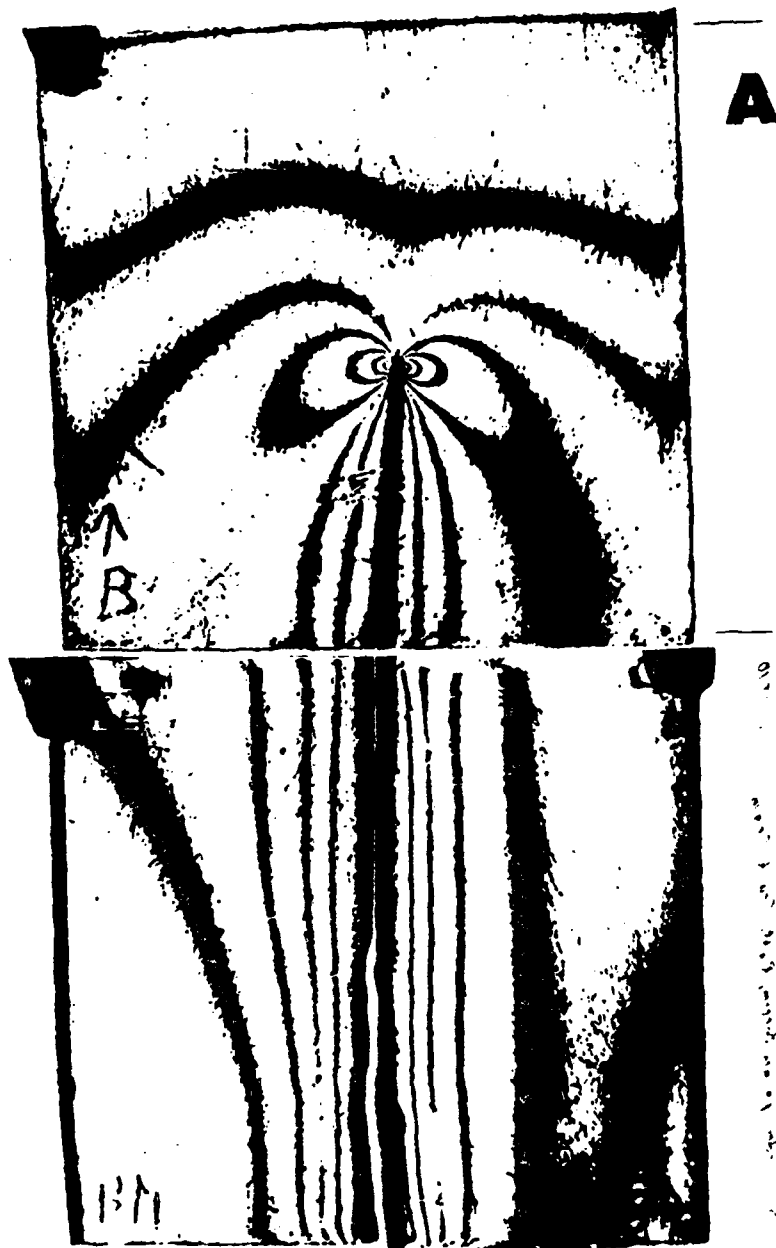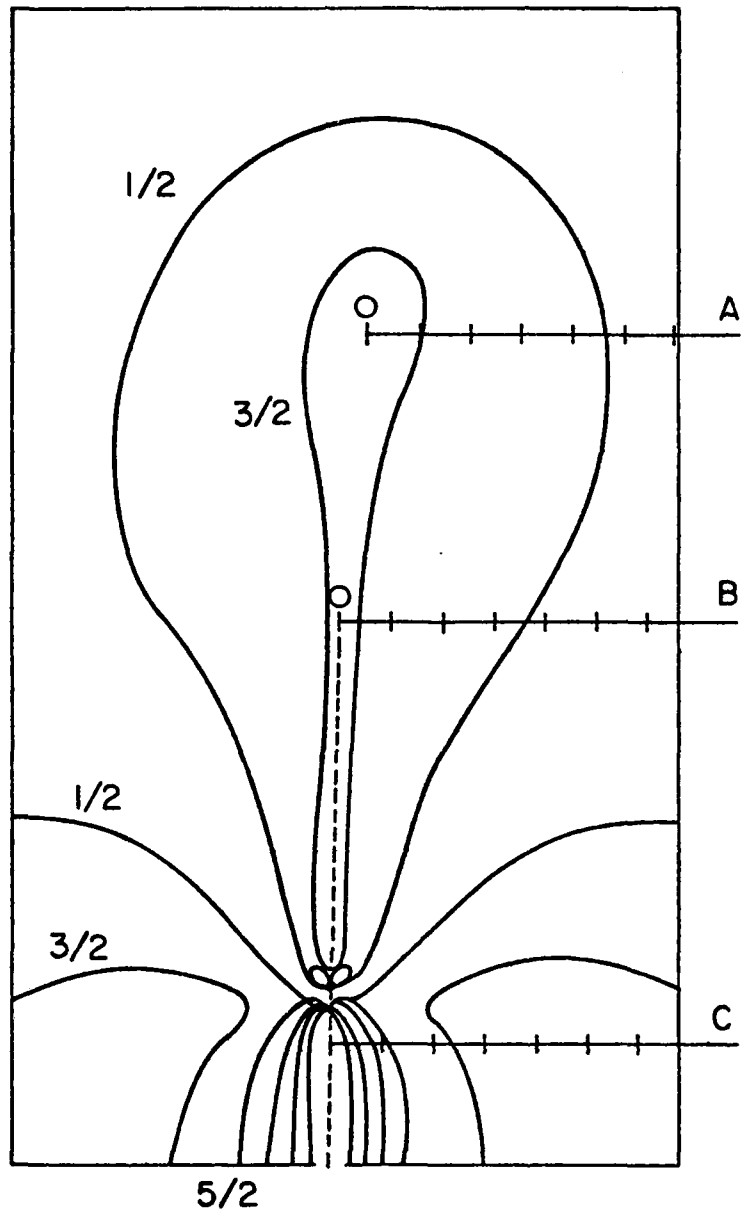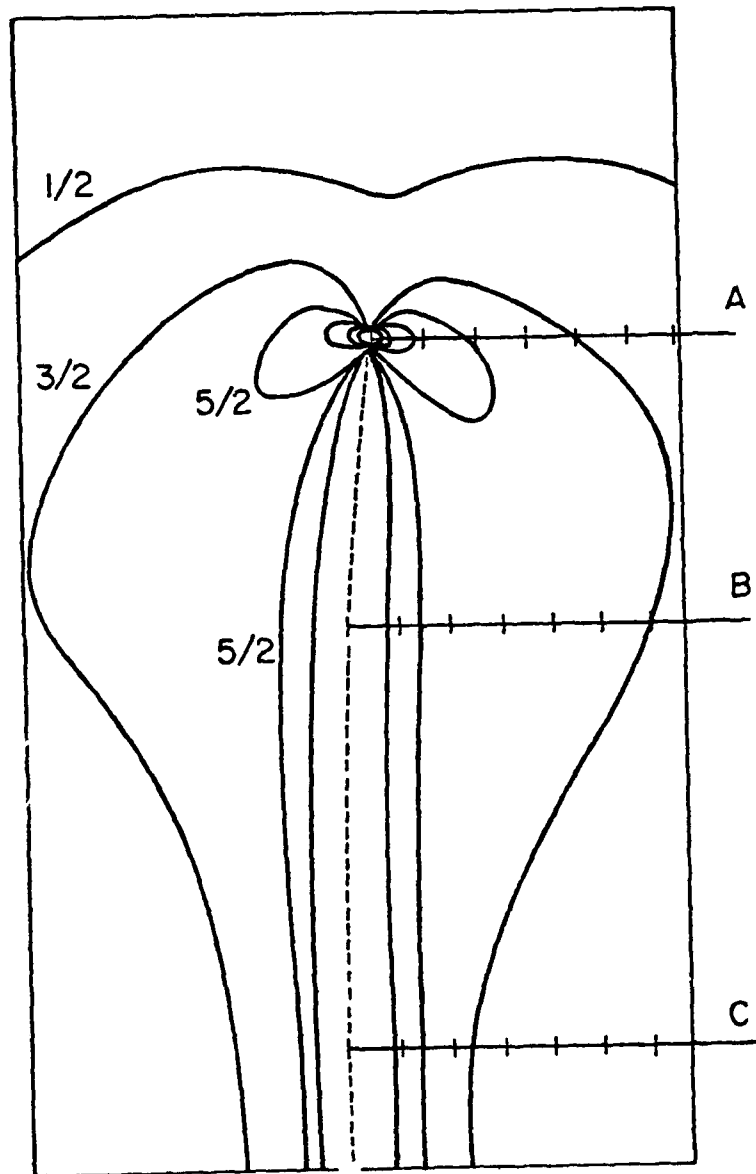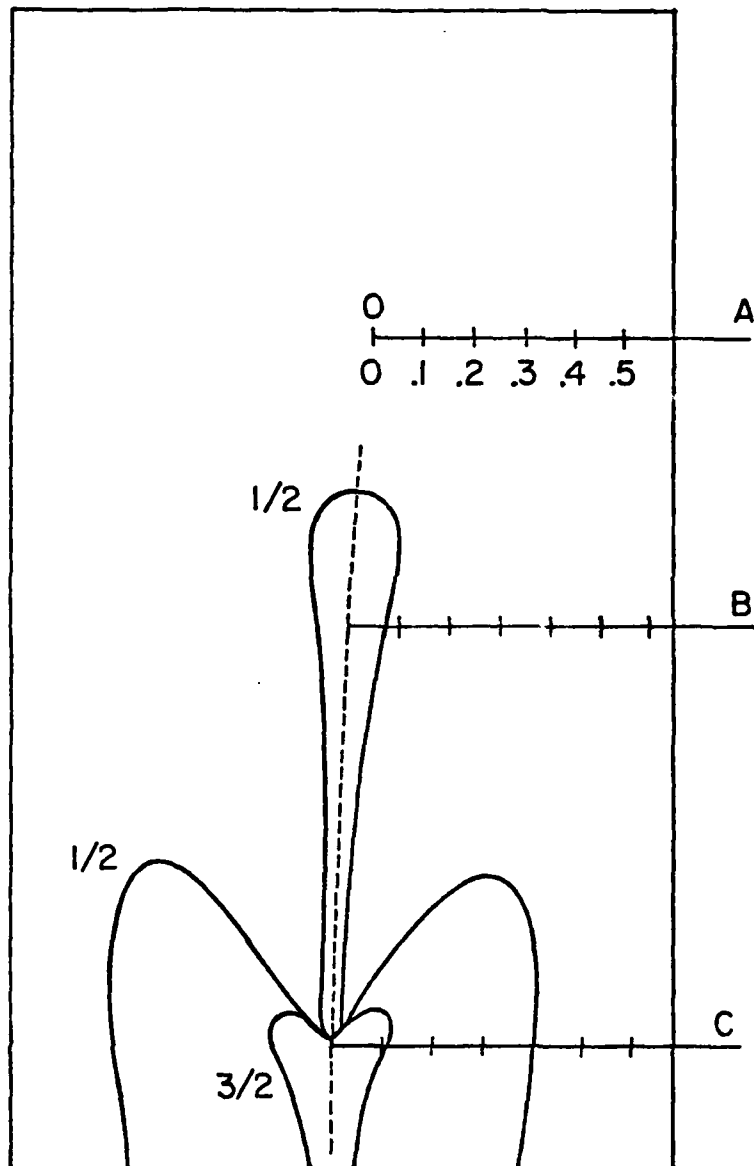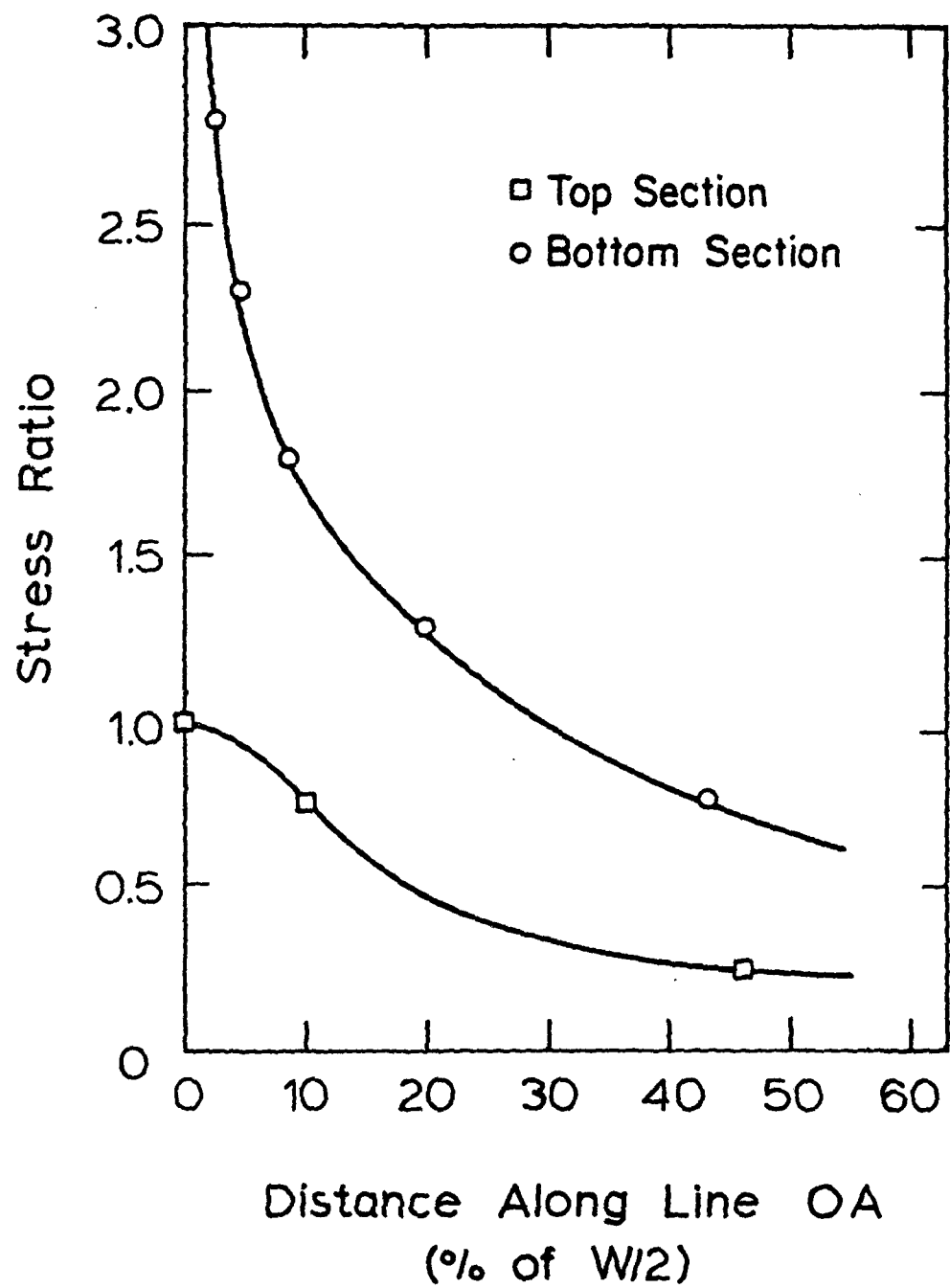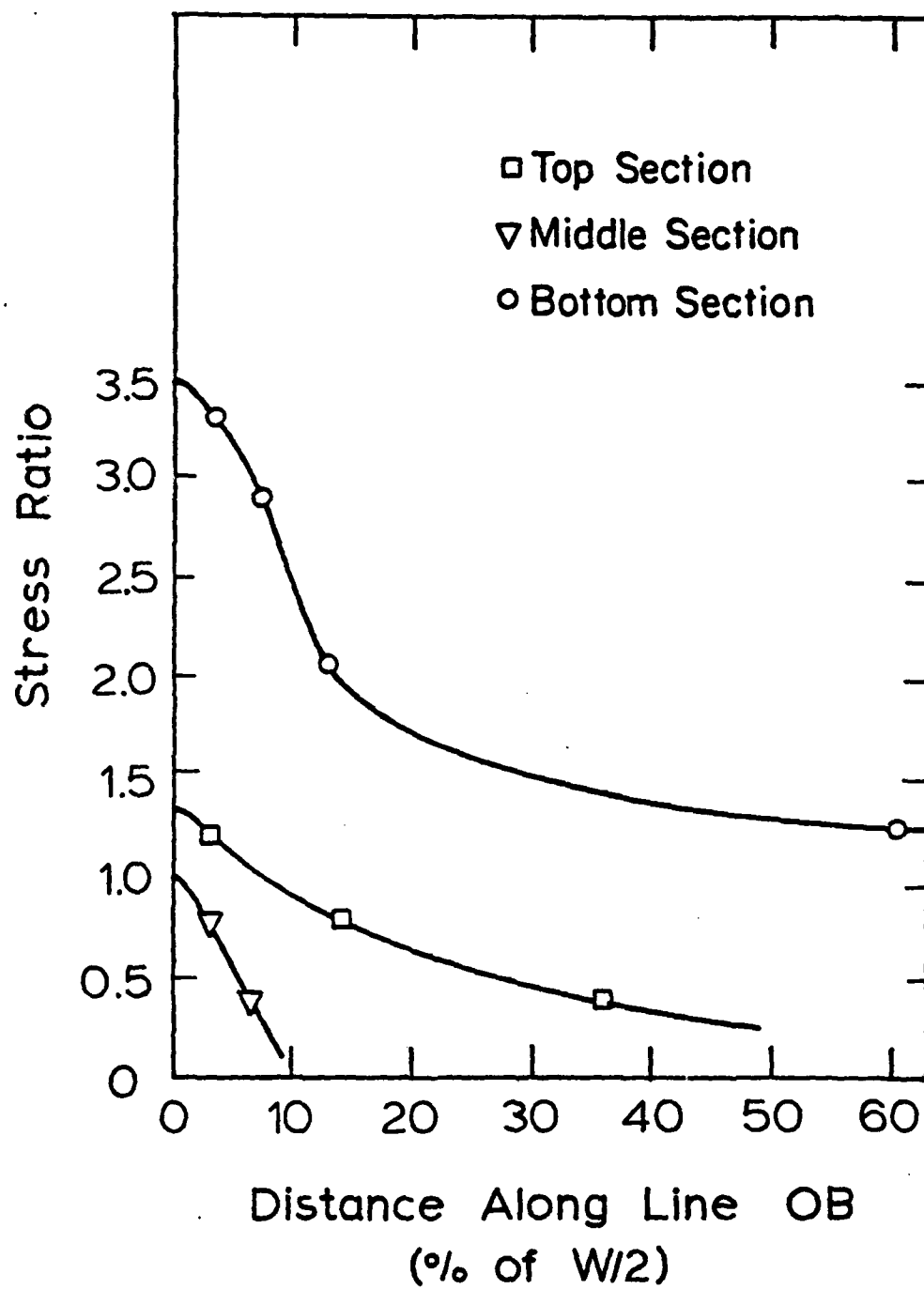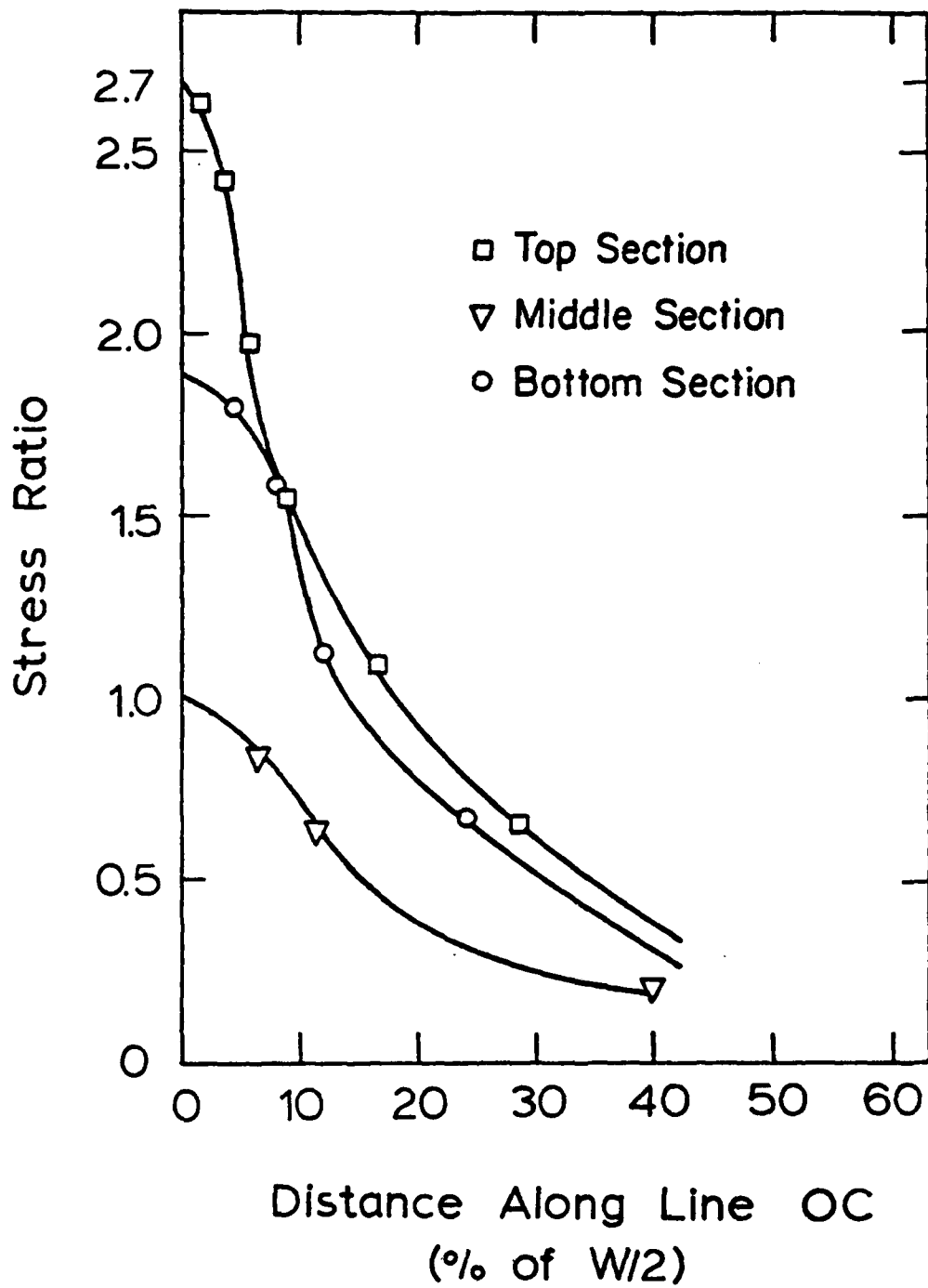
Fig. 13   B. Hindin

Fig. 14 B. Hindin

Fig. 15   B. Hindin

DATE FILMED

8